

Evaluation of the IMERG Product Performance at Estimating the Rainfall Properties in a Semi-Arid Region of Mexico

Eric Muñoz de la Torre, Julián González Trinidad, Efrén González Ramírez

Abstract—Rain varies greatly in its duration, intensity, and spatial coverage, it is important to have sub-daily rainfall data for various applications, including risk prevention, however, the ground measurements are limited by the low and irregular density of rain gauges. An alternative to this problem is the Satellite Precipitation Products (SPPs) that use passive microwave and infrared sensors to estimate rainfall, as IMERG, however, these SPPs have to be validated before their application. The aim of this study is to evaluate the performance of the IMERG: Integrated Multi-satellitE Retrievals for Global Precipitation Measurement final run V06B SPP in a semi-arid region of Mexico, using four rain gauges sub-daily data of October 2019 and June to September 2021, using the Minimum inter-event Time (MIT) criterion to separate unique rain events with a dry period of 10 hrs for the purpose of evaluating the rainfall properties (depth, duration and intensity). Point to pixel analysis, continuous, categorical, and volumetric statistical metrics were used. Results show that IMERG is capable to estimate the rainfall depth with a slight overestimation but is unable to identify the real duration and intensity of the rain events, showing moderate overestimations and underestimations, respectively. The study zone presented 80 to 85% of convective rain events, the rest were stratiform rain events, classified by the depth magnitude variation of IMERG pixels and rain gauges. IMERG showed poorer performance at detecting the first ones but had a good performance at estimating stratiform rain events that are originated by Cold Fronts.

Keywords—IMERG, rainfall, rain gauge, remote sensing, statistical evaluation.

I. INTRODUCTION

PRECIPITATION is the most basic component in the global water cycle, and it plays equally important roles in sustaining nature and human life. Precipitation drives the flow of energy through the climate and the biosphere, and it supplies society with continually renewed water resources. Many types of precipitation exist, including convective, frontal (stratiform), cyclonic, and orographic, and precipitation is affected by many factors, such as geographical location, atmospheric circulation, and the underlying land-surface conditions. More so than other water cycle elements, precipitation exhibits large spatial and temporal variation, which greatly undermines the reliability of producing reasonable precipitation estimates [1]. Studying the properties of precipitation events is important for deepening our understanding of precipitation physics and accurately modeling

precipitation-driven processes [2].

Precipitation is commonly derived from direct observations that rely on ground-based rain gauges, which can provide direct precipitation measurements from a finite set of spatial locations on land surface that are usually too sparse to represent well fine-scale spatial variations of precipitation observed in large areas. In remote areas such as deserts, mountains, and seas, where the spatiotemporal coverage of data is especially sparse, the accuracy of extreme precipitation estimations is considerably reduced [3].

However, with the rapid advancing of the remote sensing technique, various SPPs with high accuracy and resolution emerge as attractive alternatives, for example IMERG, greatly compensating the lack of in-situ observation data. Though, purely satellite-based precipitation derived from simulation or artificial intelligence is inevitably dogged by systematic or random errors due to sampling uncertainties, precipitation retrieval algorithms or surface environmental conditions. Evaluating satellite-based precipitation products is therefore an indispensable step before their applications [4].

Still, most published studies assess SPPs by lumping together all hourly or daily data and computing statistical indicators, an approach that largely erases the crucial information in the properties of individual precipitation events [2].

A series of works by Gentilucci et al., 2022 [5], Wang et al., 2023 [1], Jiang et al., 2022 [6], and Yang et al., 2020 [7], evaluated the performance of IMERG at different defined temporal scales, as half hourly, hourly, daily, monthly and annual, concluding that IMERG overestimates the rainfall depth, the precipitation detection ability of IMERG is influenced by the rainfall type and topography, the IMERG performance increases with time aggregation.

For the other hand, fewer studies, such as [8] and [2] separated the rainfall data into individual rain events to evaluate the performance of IMERG at estimating the rainfall properties, and concluded that IMERG cannot depict the duration and intensity of the rain events, because of large overestimations and underestimations respectively, but is capable of estimate the rain depth with a slight overestimation.

In this study the MIT that is an index to delineate independent storms from sub-daily rainfall records [9] is used to separate

Eric Muñoz de la Torre is with Doctorado en Ciencias de la Ingeniería, Universidad Autónoma de Zacatecas, Zacatecas, CO 98160 México (e-mail: emudelato@uaz.edu.mx).

Julián González Trinidad is with Doctorado en Ciencias de la Ingeniería, Universidad Autónoma de Zacatecas, Zacatecas, CO 98160 México

(corresponding author, phone: +52 1 492 942 0984; e-mail: jgonza@uaz.edu.mx).

Efrén González Ramírez is with Doctorado en Ciencias de la Ingeniería, Universidad Autónoma de Zacatecas, Zacatecas, CO 98160 México (e-mail: gonzalezefren@uaz.edu.mx).

individual rain events (IREs) to evaluate the performance of IMERG Final Run V06B at estimating the rainfall properties (depth, duration and intensity), using 4 rain gauges sub-daily data from October 2019 and June to September 2021 as the truth.

II. MATERIALS AND METHODS

A. Study Area

The study area has a surface of 246.86 km² inside two continuous IMERG pixels in a south-central region of the state of Zacatecas between coordinates 22.7° and 22.7° N and 102.7° and 102.6° W. The altitude varies from 2186 to 2561 meters above sea level (m.a.s.l.) (Fig. 1).

The predominant climate in most of Zacatecas is dry and semi-dry (73%); 17% of the territory, in the east of the state, is temperate subhumid; in 6% of the territory, mainly the north and northeast regions, the climate is very dry, and the remaining 4% of the state, in the south and southwest, presents subhumid warm climate. Mean annual temperature is 17 °C, with a maximum mean temperature of 30 °C in the month of May and a minimum mean temperature of 3 °C in the month of January. Average annual precipitation is 510 mm; the rainy season is presented on summer in the months of June to September. The dry and semi-dry climate of the state is a limitation for the agriculture with main crops as: corn, oats, wheat, beans, chili, sorghum, nopal and peach [10].

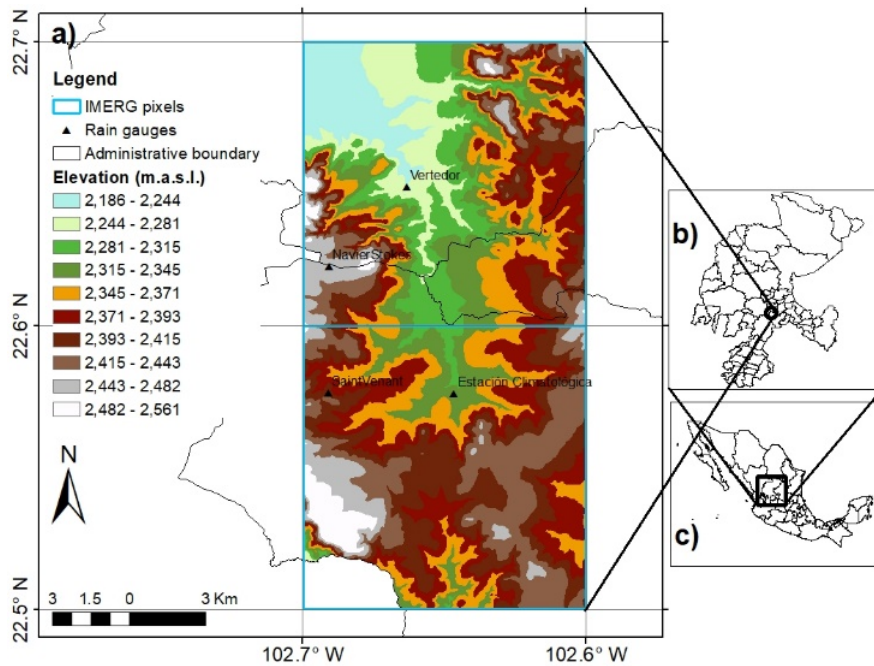


Fig. 1 Map of (a) study area, (b) state of Zacatecas, and (c) Mexico country

B. Ground Observed Rainfall Data

The observed sub-daily rainfall data from 2019 to 2021 were collected from 4 rain gauges of the Universidad Autónoma de Zacatecas (UAZ) (Table I). Only the data of the rain season (June to September, sometimes October) were selected for the present work. The data were aggregated to match with the IMERG temporal resolution of half hour. The data were none of the rain gauges or IMERG pixels measured or estimated rainfall were eliminated. Finally, the data used for the analysis were from October 2019, and June to September 2021.

A MIT of 10 hrs that is recommended for storm-based studies [9] was selected to identify IREs according to the observed data, and this where compared against IMERG data.

The rain events were classified in convective and stratiform events, according to the rainfall depth variation measured or estimated between the rain gauges and the IMERG pixels, the convective rain events were those were at least one of the two rain gauges that share the same pixel or that pixel, recorded a rain depth twice or greater than the others, so the stratiform

events were those with greatest similarity in rainfall depth records.

TABLE I
RAIN GAUGES AND THEIR LOCATIONS

Rain gauge	Latitude	Longitude	Elevation (m.a.s.l.)
Estación Climatológica (EC)	22.58°	102.65°	2323
NavierStokes (NS)	22.62°	102.69°	2464
SaintVenant (SV)	22.58	102.69°	2403
Vertedor (V)	22.65°	102.66°	2248

C. IMERG Estimated Rainfall Data

IMERG, with a high spatial resolution of 0.1°, a wide coverage of 90° S/N (full 60° S/N), and a short temporal resolution (0.5 hrs), was generated by the National Aeronautics and Space Administration and used the IMERG algorithm to intercalibrate, unite, and merge all precipitation estimates. The recent IMERG version 06 (V06) product, with a temporal period starting from June 2000, was retrospectively processed in the TRMM era and has proven highly capable in estimating

light and solid precipitations. Currently, IMERG has undertaken a project to replace TMPA datasets, and it has gradually come to be utilized in relevant precipitation studies. The post-real-time IMERG Final Run product provides the closest estimates to the actual precipitation data in the IMERG suite of products and is calibrated using the Global Precipitation Climatological Centre (GPCC) monthly gauge analysis data [6].

In this research, the GPM IMERG Final Precipitation L3 Half Hourly 0.1° x 0.1° V06 (GPM_3IMERGHH) data were downloaded from the GES DISC (Goddard Earth Sciences Data and Information Services Center) web page (<https://disc.gsfc.nasa.gov/>). The time of the IMERG data (UTC) were corrected to the local time (UTC-6). The two IMERG pixels of interest for this study were selected and extracted using Python 3.11 [11] to match with the rain gauges locations (Fig. 1).

D. Statistical Analysis

The performance of the IMERG product at estimating the rainfall properties depth, duration and rain intensity was quantitatively analyzed with respect to continuous statistical measurement, categorical metrics, and volumetric indices. The continuous statistics used to measure the difference between satellite estimates and observations included the relative bias (Bias), correlation coefficient (r), mean error (ME), and root mean square error (RMSE). Bias, r , ME, and RMSE values were calculated using the following equations [3], [4], [6], [12]:

$$Bias = \frac{\sum_{i=1}^N (S_i - G_i)}{\sum_{i=1}^N (G_i)} \quad (1)$$

$$r = \frac{\sum_{i=1}^N (S_i - \bar{S})(G_i - \bar{G})}{\sqrt{\sum_{i=1}^N (S_i - \bar{S})^2} \sqrt{\sum_{i=1}^N (G_i - \bar{G})^2}} \quad (2)$$

$$ME = \frac{1}{N} \sum_{i=1}^N (S_i - G_i) \quad (3)$$

$$RMSE = \sqrt{\frac{1}{N} \sum_{i=1}^N (S_i - G_i)^2} \quad (4)$$

where S_i represents satellite rainfall estimates, G_i is the ground-based rainfall observation, \bar{S} is the average of satellite rainfall estimates, \bar{G} indicates the average of ground-based rainfall observations, N represents the total number of data, and i is the number of the sample.

Bias is the overall deviation of SPPEs from gauge observations, which indicates over- or underestimation. The correlation coefficient describes the degree of linear correspondence between satellite estimates and ground-based observations. The ME describes the average disparity between SPPEs and ground-based observations. RMSE represents the average error between SPPEs and ground measurement. A value of 0 is the deal score for bias, ME, and RMSE, and a value of 1 is the highest correlation coefficient value.

The categorical metric was used to determine the abilities of satellite products for the occurrence of rainfall scenario. These statistics were extracted from a 2×2 contingency table in which

the number of hits (H) describes the number of correctly estimated rain events from satellite and ground-based observation, false alarm (F) refers to when rain is estimated but no rain actually occurs, miss (M) refers to when rain is not estimated by the satellite but rain actually occurs, and correct negative (CN) refers to true null events (Table II). Three statistical parameters were adopted, namely the probability of detection (POD), false alarm ratio (FAR), and critical success index (CSI). POD score defines the ability of the satellite products to correctly estimate rain events. FAR measures how often the satellite products detect rainfall not confirmed by ground observation. CSI is also known as a threat score and computes the ratio of all events estimated and observed that were correctly diagnosed. The perfect value for POD and CSI is 1, whereas that for FAR is 0. The POD, FAR, and CSI values were examined using the following formulas [3], [4], [12]:

$$POD = \frac{H}{H+M} \quad (5)$$

$$FAR = \frac{F}{H+F} \quad (6)$$

$$CSI = \frac{H}{H+M+F} \quad (7)$$

TABLE II
 CONTINGENCY TABLE FOR CATEGORICAL METRICS

		Ground observation	
		Yes	No
Satellite estimates	Yes	H	F
	No	M	CN

However, the categorical metric does not provide any information on the volume of the variable detected correctly/incorrectly; therefore, this study adopted volumetric indices for the evaluation of data. Volumetric indices provide the volume of the variable of interest detected correctly by SPPEs relative to rain gauge observations. In this study, we used the volumetric hit index (VHI), volumetric false alarm ratio (VFAR), and volumetric critical success index (VCSI). VHI is defined as the volume of rainfall accurately detected by SPPEs relative to the volume of the accurately detected satellite and missed observations. VFAR can be expressed as the volume of false rainfall detected by the SPPEs relative to the sum of rainfall detected by the SPPEs. VCSI is defined as an overall measure of volumetric performance. VHI, VFAR, and VCSI range from 0 to 1, with the perfect score for VHI and VCSI being 1 and for VFAR, 0. The equations for volumetric indices are as follows [12]:

$$VHI = \frac{\sum_{i=1}^N (S_i | (S_i > t \& G_i > t))}{\sum_{i=1}^N (S_i | (S_i > t \& G_i > t)) + \sum_{i=1}^N (G_i | (S_i \leq t \& G_i > t))} \quad (8)$$

$$VFAR = \frac{\sum_{i=1}^N (S_i | (S_i > t \& G_i \leq t))}{\sum_{i=1}^N (S_i | (S_i > t \& G_i > t)) + \sum_{i=1}^N (S_i | (S_i > t \& G_i \leq t))} \quad (9)$$

$$VCSI = \frac{\sum_{i=1}^N (S_i | (S_i > t \& G_i > t))}{\sum_{i=1}^N (S_i | (S_i > t \& G_i > t)) + \sum_{i=1}^N (G_i | (S_i \leq t \& G_i > t)) + \sum_{i=1}^N (S_i | (S_i > t \& G_i \leq t))} \quad (10)$$

where t indicates a threshold value of 2.5 mm/event, to exclude events deemed insignificant, this threshold matches with other study that evaluated IREs [8].

The categorical and volumetric metrics were only applied to the depth rainfall property.

III. RESULTS

A. Analysis of the Half Hour Temporal Resolution Rainfall Data

In the half hour temporal resolution, the IMERG data tended to underestimate the intensity and overestimate the duration of the rain events (Fig. 2), the latter is because IMERG is estimating rainfall when the rain gauges are not.

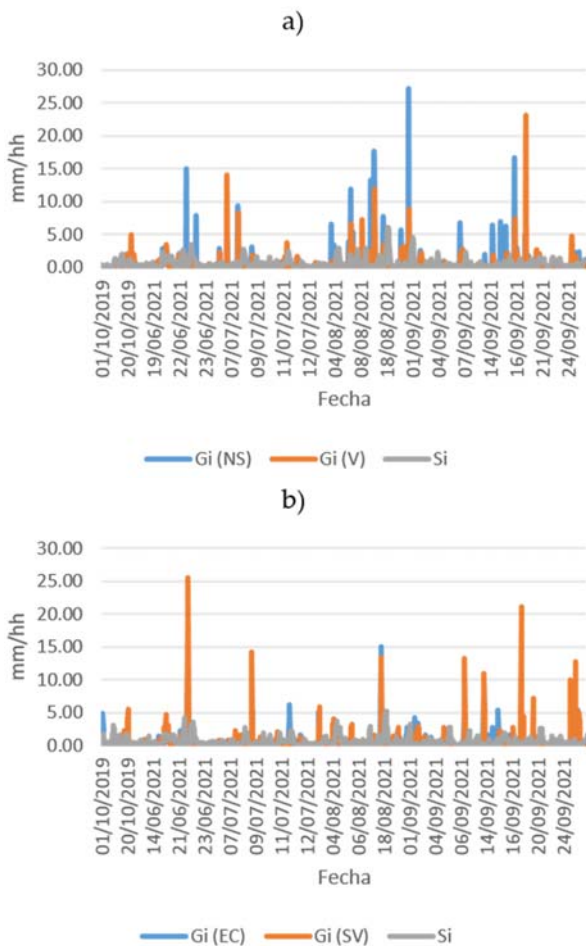


Fig. 2 Comparison between the IMERG and the rain gauges data at half hour temporal resolution: (a) and (b) are the two IMERG pixels with their respective rain gauges

B. Assessment of the Rainfall Properties of the IREs

The half hourly data were aggregated into IREs with a MIT of 10 hours. Resulting in 63 IREs, these were classified into convective and stratiform rain events, depending in the

variation of the measurements between the IMERG and the rain gauge data. 80 to 85% of the IRE were convective and the rest stratiform.

The IMERG data showed a slight and moderate overestimation of the rainfall depth and duration of the IREs respectively, the greater overestimation of the duration caused that IMERG tended to underestimate the rain intensity, The stratiform rain events had higher depth and duration than the convective rain events with a mean of 10-16 mm/event and 10-21 h, the intensity of all the rain events had a mean near to 1 mm/h, with heavy intensity events up to 15 to 18 mm/h recorded by the rain gauges in the convective rain events (Fig. 3).

According to the bias evaluation of IMERG, the convective rain events showed higher overestimation of depth and duration than the stratiform rain events ranging in 0.2-1 and 1.2-1.8 respectively, meanwhile the generally underestimated rain intensity remained nearly unchanged with the exception that the SPP overestimated the rain intensity of the convective events recorded by Saint Venant (Fig. 4).

The stratiform rain events showed a higher correlation coefficient between the IMERG and the rain gauge data in all rainfall properties ranging in 0.65 to 0.85 with depth and duration, however the intensity property had low r values ranging in 0.21-0.79 with the higher values obtained between the IMERG, NavierStokes and Vertedor data with r values of 0.6 to 0.8 (Fig. 4).

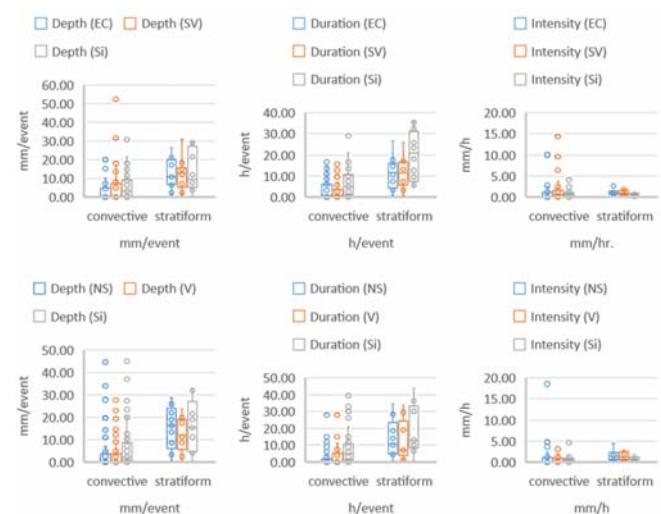


Fig. 3 IMERG and rain gauge rainfall properties data of the IREs through convective and stratiform rain events

The error values of the depth were smaller in the stratiform events and with the NavierStokes and Vertedor rain gauges, this matches with the rain intensity correlation coefficient, however these values were larger with the duration, this could be because the stratiform rain events have a larger duration than the convective rain events, the error metrics of the rain intensity remained low and nearly unchanged, due to the intensity magnitudes were generally low in all rain events (Fig. 4).

The detection ability of IMERG at estimating the rain depth was better with the stratiform rain events, showing perfect

values of POD, and nearly perfect values of CSI (0.88-1), VHI (0.96-1), and VCSI (0.96-0.98), besides the FAR and VFAR obtained values were very small ranging in 0.09-0.12 and 0.01-0.02 respectively, for the other hand with the convective rain events the FAR and VFAR values had a range of 0.4-0.5 and 0.21-0.31 respectively, this combined with the missed rain events originated lower CSI and VCSI values than the stratiform rain events (Fig. 5).

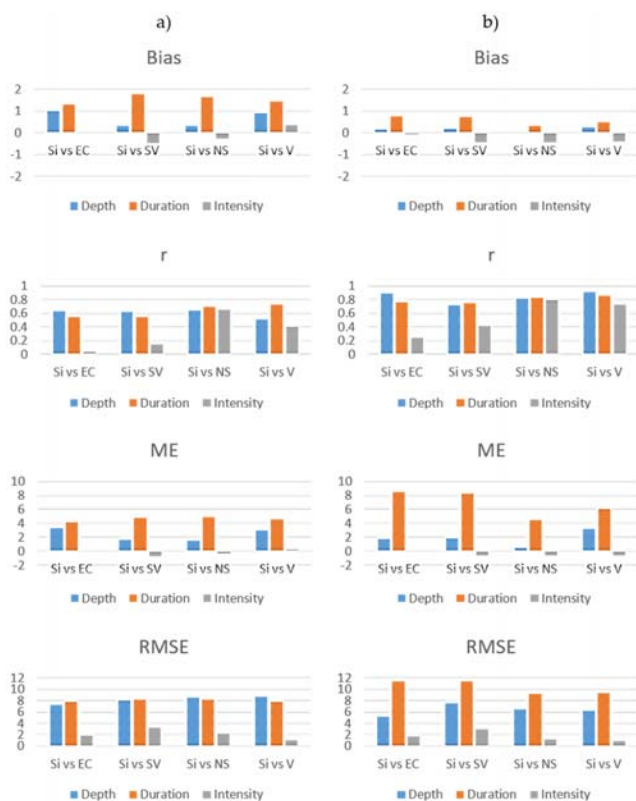


Fig. 4 Continuous statistical metrics in the rainfall properties evaluation: (a) convective and (b) stratiform IREs

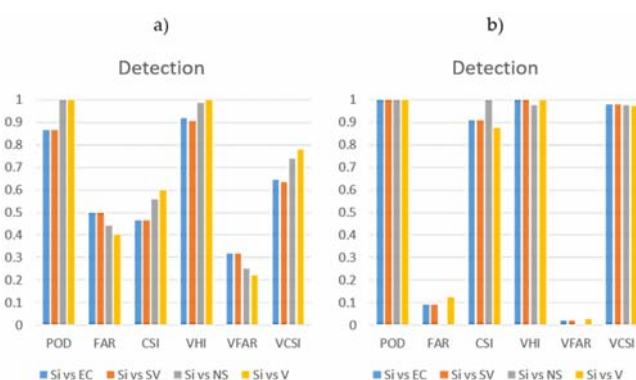


Fig. 5 Categorical and volumetric statistical metrics in the rainfall depth evaluation: (a) convective and (b) stratiform IREs

IV. CONCLUSION

63 IREs were identified using a MIT of 10 h. The 80-85% of the IREs were classified as convective and the rest as stratiform rain events, according to the variation of the depth recorded by

the IMERG and the rain gauge data.

The IMERG product obtained satisfactory performance results especially at estimating the rainfall properties of the stratiform IREs, this could be because IMERG estimates the average rainfall in an area of $0.1 \times 0.1^\circ$, and the rain gauges measure punctually.

The depth and duration of all the IREs were slightly and moderately overestimated respectively, for that reason the rain intensity was underestimated.

The detection ability of IMERG was very good in both kinds of rain, but the stratiform events obtained FAR values near to 0, meanwhile the convective obtained large FAR values, this affected the CSI.

Using a denser rain gauge network could be beneficial to see if the differences in the performance of IMERG at estimating the rainfall properties through convective and stratiform rain events are still high in future work.

REFERENCES

- [1] Y. Wang, C. Miao, X. Zhao, Q. Zhang, and J. Su, "Evaluation of the GPM IMERG product at the hourly timescale over China," *Atmospheric Res.*, vol. 285, p. 106656, Apr. 2023, doi: 10.1016/j.atmosres.2023.106656.
- [2] R. Li, C. Guilloteau, P.-E. Kirstetter, and E. Foufoula-Georgiou, "How well does the IMERG satellite precipitation product capture the timing of precipitation events?," *J. Hydrol.*, vol. 620, p. 129563, May 2023, doi: 10.1016/j.jhydrol.2023.129563.
- [3] L. Yu, G. Leng, and A. Python, "A comprehensive validation for GPM IMERG precipitation products to detect extremes and drought over mainland China," *Weather Clim. Extrem.*, vol. 36, p. 100458, Jun. 2022, doi: 10.1016/j.wace.2022.100458.
- [4] P. Weng, Y. Tian, Y. Jiang, D. Chen, and J. Kang, "Assessment of GPM IMERG and GSMaP daily precipitation products and their utility in droughts and floods monitoring across Xijiang River Basin," *Atmospheric Res.*, vol. 286, p. 106673, May 2023, doi: 10.1016/j.atmosres.2023.106673.
- [5] M. Gentilucci, M. Barbieri, and G. Pambianchi, "Reliability of the IMERG product through reference rain gauges in Central Italy," *Atmospheric Res.*, vol. 278, p. 106340, Nov. 2022, doi: 10.1016/j.atmosres.2022.106340.
- [6] S. Jiang, L. Wei, L. Ren, L. Zhang, M. Wang, and H. Cui, "Evaluation of IMERG, TMPA, ERA5, and CPC precipitation products over mainland China: Spatiotemporal patterns and extremes," *Water Sci. Eng.*, vol. 16, no. 1, pp. 45-56, Mar. 2023, doi: 10.1016/j.wse.2022.05.001.
- [7] M. Yang, G. Liu, T. Chen, Y. Chen, and C. Xia, "Evaluation of GPM IMERG precipitation products with the point rain gauge records over Sichuan, China," *Atmospheric Res.*, vol. 246, p. 105101, Dec. 2020, doi: 10.1016/j.atmosres.2020.105101.
- [8] E. da S. Freitas *et al.*, "The performance of the IMERG satellite-based product in identifying sub-daily rainfall events and their properties," *J. Hydrol.*, vol. 589, p. 125128, Oct. 2020, doi: 10.1016/j.jhydrol.2020.125128.
- [9] W. Wang *et al.*, "Minimum Inter-Event Times for Rainfall in the Eastern Monsoon Region of China," *Trans. ASABE*, vol. 62, no. 1, pp. 9-18, 2019, doi: 10.13031/trans.12878.
- [10] INEGI, "Resumen de Zacatecas." Accessed: Feb. 27, 2023. Online. Available: <https://cuentame.inegi.org.mx/monografias/informacion/zac/>
- [11] G. Van Rossum and F. L. Drake, *Python 3 Reference Manual*. Scotts Valley, CA: CreateSpace, 2009.
- [12] C.-Y. Liu, P. Aryastana, G.-R. Liu, and W.-R. Huang, "Assessment of satellite precipitation product estimates over Bali Island," *Atmospheric Res.*, vol. 244, p. 105032, Nov. 2020, doi: 10.1016/j.atmosres.2020.105032.